

Tau-pair Performance in ILD Detectors

Taikan Suehara¹, Akiya Miyamoto², Keisuke Fujii²,
Nobuchika Okada², Hideo Ito³,
Katsumasa Ikematsu² and Ryo Yonamine⁴

- 1- The University of Tokyo - International Center for Elementary Particle Physics (ICEPP)
7-3-1 Hongo, Bunkyo-ku, Tokyo, 113-0033, Japan
- 2- High Energy Accelerator Research Organization (KEK)
- Institute of Particle and Nuclear Studies (IPNS)
1-1 Oho, Tsukuba, Ibaraki, 305-0801, Japan
- 3- The University of Tokyo - Institute for Cosmic Ray Research (ICRR)
5-1-5 Kashiwa-no-ha, Kashiwa, Chiba, 277-8582, Japan
- 4- The Graduate University for Advanced Studies (SOKENDAI)
- School of High Energy Accelerator Science
1-1 Oho, Tsukuba, Ibaraki, 305-0801, Japan

Tau-pair process has been analyzed in the ILD detector model as a benchmark process for LoI. Results of background rejection, forward-backward asymmetry and polarization measurements are obtained with full detector simulation. Impact of detector parameters for tau-pair analysis is also discussed in this paper.

1 Motivations of tau-pair study

Tau-pair process ($e^+e^- \rightarrow Z^* \rightarrow \tau^+\tau^-$) at $\sqrt{s} = 500$ GeV is one of the benchmark processes[2] proposed by Research Director. According to the report, this process is a good sample to examine detector performances of

- tau reconstruction, aspects of particle flow,
- π_0 reconstruction,
- tracking of very close-by tracks.

In this process, tau leptons are highly boosted ($\gamma \sim 140$), thus decay daughters (mainly charged and neutral pions, muons and electrons) are concentrated in a very narrow angle. Reconstruction of π_0 from two photons is especially challenging for the ILC detectors, and much depends on detector parameters, so it is a good measure for detector optimization.

Required observables are cross section, forward-backward asymmetry and polarization of tau leptons. The polarization measurement requires identification of tau decays, including reconstruction of π_0 . Efficiency and purity of event selection cuts should also be used for comparison of detector performances.

For physics motivation, tau-pair process is important as a precision measurement of the electroweak theory. For example, measuring cross section and forward-backward asymmetry of tau-pair process very precisely can probe existence of heavy Z' boson.

Geometry	gldapr08_14m	gldprim_v04	j4ldc_v04	LDCPrime_02Sc
Software	Jupiter	Jupiter	Jupiter	Mokka
Magnetic field	3 Tesla	3.5 Tesla	4 Tesla	3.5 Tesla
TPC R_{\min}	43.7 cm	43.5 cm	34.0 cm	37.1 cm
ECAL R_{\min}	210 cm	185 cm	160 cm	182.5 cm
ECAL thickness	19.8 cm	19.8 cm	19.8 cm	17.2 cm
HCAL thickness	120 cm	109 cm	96 cm	127.2 cm
ECAL granularity	1x1 cm	1x1 cm	1x1 cm	0.5x0.5 cm

Table 1: Detector geometries used in this study.

2 Analysis framework and events

2.1 Monte Carlo simulation and detector geometries

The ILD group has two full detector simulation models, Mokka and Jupiter. Mokka originates in LDC detector and Jupiter originates in GLD detector, and both are based on Geant4 Monte Carlo simulation. In this study I used both simulation models. Mokka has geometries with detailed implementation of detector components. I used simulated events processed in Mokka LDCPrime_02Sc geometry. The ILD group has simulated quite a large fraction of full Standard Model (SM) samples, required in the benchmark report, in LDCPrime_02Sc geometry and I used the events to estimate and optimize background suppression. In contrast, Jupiter has relatively rough geometries and full SM samples have not been processed, but we have tau-pair samples in several Jupiter geometries with three detector parameters, gldapr08_14m, gldprim_v04, j4ldc_v04. Summary of detector geometries is shown in Fig. 1. In rough summary, three geometries in Jupiter differ in sizes, gldapr08_14m is large, gldprim_v04 is middle, j4ldc_v04 is small in size. Magnetic field is such that BR for each geometry is almost the same. LDCPrime_02Sc is almost as same as gldprim_v04 in size, but it has a finer ECAL granularity of 0.5x0.5 cm. Detailed geometry is much different between Jupiter and Mokka geometries.

For event reconstruction, including smearing of tracker and calorimeter hits, tracking, clustering and particle flow, I used MarlinReco framework with PandoraPFA particle flow algorithm. Raw output of Jupiter is not compatible with MarlinReco LCIO format, but we have a converter to obtain LCIO files of Jupiter events. PandoraPFA is especially optimized for Mokka geometries, so particle flow performance of Jupiter is slightly worse.

2.2 Event samples

For signal tau-pair events, we use events generated in DESY. Whizard 1.51 and TAUOLA are used to generate the events. SLAC standard samples for LoI are not used because of polarization issues. I used 80 fb^{-1} signal sample of each geometry for A_{FB} and polarization analysis without background. For background study, SLAC standard samples are used. All events simulated in LDCPrime_02Sc geometry, about 20 million events in total, are processed with my analysis cuts.

Integrated luminosity is assumed to be 500 fb^{-1} each for two polarization setups, $e_L^- e_R^+$ and $e_R^- e_L^+$. Assumed polarization ratio is 80% for electron and 30% for positron (i.e. for $e_L^- e_R^+$ setup 90% of electrons are leftly polarized and 65% of positrons are rightly polarized).

2.3 Tau clustering

For tau clustering, an original clustering processor (TaJet) is applied to the output of PandoraPFA. Following is a procedure of the processor.

1. Sort particles in energy order.
2. Select the most energetic charged particle (a tau candidate).
3. Search particles to be associated to the tau candidate. Criteria is:
 - (a) Opening angle to the tau candidate is smaller than 50 mrad., or
 - (b) Opening angle to the tau candidate is not larger than 1 rad. and invariant mass with the tau candidate is less than 2 GeV ($m_\tau = 1.777$ GeV).
4. Combine energy and momentum of the tau candidate and associated particle and treat the combined particle as the new tau candidate.
5. Repeat from 3.
6. After all remaining particles do not meet the criteria, remaining most energetic charged particle is the next tau candidate. (Repeat from 2.)
7. After all charged particles are associated to tau candidates, remaining neutral particles are independently included in the cluster list as neutral fragments.

In the clustering stage, events with > 6 tracks are pre-cut to accelerate clustering since $> 99\%$ of tau decays have ≤ 3 charged particles. Event with only one positive and one negative tau clusters are processed with latter analysis.

3 Background suppression

Main background of tau-pair analysis is Bhabha ($e^+e^- \rightarrow e^+e^-$), $WW \rightarrow \ell\nu\ell\nu$ and $\gamma\gamma \rightarrow \tau^+\tau^-$. Since cross sections of Bhabha and two-photon events are huge (about 10^4 and 10^3 larger than signal, respectively), we need tight selection cuts for those background events. Following cuts are applied to signals and all SM background events after the tau clustering.

1. Number of tracks ≤ 6 . Included as a pre-cut in tau clustering processor.
2. Only one positive and one negative tau clusters must exist in the event.
3. Opening angle of two tau candidates must be > 178 deg.
This cut efficiently suppresses $WW \rightarrow \ell\nu\ell\nu$ background.
4. ee and $\mu\mu$ events are rejected.

Charged particles depositing $> 90\%$ of their energy in ECAL are identified as electrons, and charged particles depositing $< 70\%$ of their energy (estimated by curvature of their tracks) in ECAL+HCAL are identified as muons. Events with two electrons or two muons are rejected in this cut. This cut is especially for suppressing Bhabha and $e^+e^- \rightarrow \mu^+\mu^-$ events. Signal loss is about 6%.

5. $|\cos\theta| < 0.9$ for both tau clusters.

t-channel Bhabha events are almost completely suppressed by this cut. 20% of signal events are lost.

6. $40 < E_{\text{vis}} < 450$ GeV.

Lower bound suppresses $\gamma\gamma \rightarrow \tau^+\tau^-$ events, and upper bound suppresses Bhabha events. Signal lost is negligibly small.

Table 2 shows the result of these cuts. $\gamma\gamma \rightarrow \tau^+\tau^-$ background is currently not included, but generator-level study shows the effect of the $\gamma\gamma \rightarrow \tau^+\tau^-$ background is not significant (most events are eliminated by the E_{vis} cut). Number of events are normalized to 500 fb^{-1} . $e_L^-e_R^+$ polarization (80% and 30%, respectively) is assumed. In total, number of background events is about 10% of signal, not significant. If we assume that we know the shape of the background, statistical error of the background is much smaller than signal statistics and negligible for the further study. $\gamma\gamma \rightarrow \tau^+\tau^-$ background is planned to be included in the LoI study.

Cuts	Signal	Background
# tracks, # clusters	5.7×10^5	7.9×10^8
Opening angle > 178 deg.	1.6×10^5	1.3×10^8
$ \cos\theta < 0.9$	1.3×10^5	1.2×10^7
ee, $\mu\mu$ veto	1.2×10^5	6.2×10^5
$45 < E_{\text{vis}} < 450$	1.2×10^5	1.3×10^4

Table 2: Cut statistics for background suppression.

4 Forward-backward asymmetry

Figure 1 shows a simulated result on angular distribution of τ^+ leptons in LD-CPrime_02Sc model. All events passed criteria described in the previous section are put into the histograms. Clear asymmetry can be seen in signal distribution. There are several bins where background is very large, but this is a result of low MC statistics of Bhabha, $\gamma^*\gamma^*$ and $e\gamma^*$ processes (about 0.1 fb^{-1} each). We plan to improve MC statistics of those events by applying preselections at generator level.

Forward-backward asymmetry can be calculated by

$$A_{FB} = \frac{N_F - N_B}{N_F + N_B}, \quad (1)$$

$$\delta A_{FB} = \frac{2\sqrt{N_F N_B (N_F + N_B)}}{(N_F + N_B)^2}, \quad (2)$$

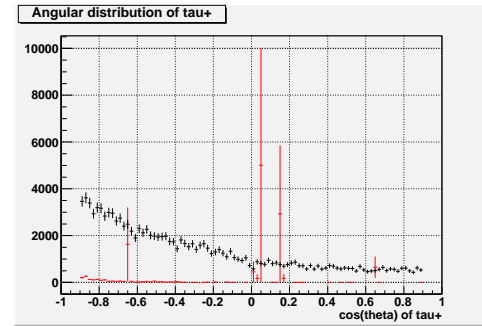


Figure 1: Angular distribution of τ^+ momentum direction. Black crosses show signal and red crosses show background. Vertical axis is normalized to 500 fb^{-1} . Error bars represent errors in current MC statistics.

where N_B is number of events in backward region ($\cos\theta < 0$) and N_F is number of events in forward region ($\cos\theta > 0$). By estimated number of signal events ($N_F = 8956, N_B = 2893$), A_{FB} is estimated to be $51.2 \pm 0.25\%$ (background statistics is not included). Since total estimated number of background events is about 10% of signal, effect of background to statistical error is smaller than signal statistics if background distribution can be well determined.

5 Polarization analysis

5.1 Event selection

There are five dominant decay modes of tau leptons, $\tau^+ \rightarrow e^+ \bar{\nu}_e \nu_\tau$ (17.9%), $\tau^+ \rightarrow \mu^+ \bar{\nu}_\mu \nu_\tau$ (17.4%), $\tau^+ \rightarrow \pi^+ \nu_\tau$ (10.9%), $\tau^+ \rightarrow \rho^+ \nu_\tau \rightarrow \pi^+ \pi^0 \nu_\tau$ (25.2%), and $\tau^+ \rightarrow a_1^+ \nu_\tau \rightarrow \pi^+ \pi^0 \pi^0 \nu_\tau$ (9.3%).

Since first two modes are leptonic 3-body decay and polarization information is partially lost due to the missing neutrinos, and the last a_1 mode has relatively low branching ratio, we currently use only $\tau^+ \rightarrow \pi^+ \nu_\tau$ and $\tau^+ \rightarrow \rho^+ \nu_\tau$ modes. These modes are selected by following criteria.

1. Tau clusters with one charged tracks are selected.
2. Clusters with electrons and muons are eliminated. Muon identification is the same as that in SM suppression cut. Electron identification is ECAL deposit $> 90\%$ for $\tau^+ \rightarrow \pi^+ \nu_\tau$ selection and $> 97\%$ for $\tau^+ \rightarrow \rho^+ \nu_\tau$ selection.
3. Clustered with energy > 10 GeV is eliminated (since lepton identification is currently poor in low energy clusters).
4. Check whether neutral particles are associated in the cluster. If > 1 GeV neutral particles are not associated, the cluster is treated as a $\tau^+ \rightarrow \pi^+ \nu_\tau$ event. If > 10 GeV neutral particles are associated, the cluster is treated as a $\tau^+ \rightarrow \rho^+ \nu_\tau$ event candidate.
5. For $\tau^+ \rightarrow \rho^+ \nu_\tau$ candidates, invariant mass of ρ is calculated from 4-momenta of charged pion and whole cluster. Clusters with invariant mass around 200 MeV to m_ρ (570 to 970 MeV) are accepted.
6. Optional π^0 mass cut is applied to the $\tau^+ \rightarrow \rho^+ \nu_\tau$ candidates. In this cut, invariant mass of π^0 is calculated with clusters which have ≥ 2 neutral particles. Events with invariant mass of 0 to 200 MeV ($m_\pi^0 = 135$ MeV) are accepted. All events with only one neutral particle are eliminated by this cut (if applied).

Figure 2 and 3 shows invariant mass distribution of ρ and π^0 with gldapr08_14m (noted GLD in the plot), gldprim_v04 (GLD'), j4ldc_v04 (J4LDC) and LDCPrime_02Sc (LDC') geometries. Especially π^0 invariant mass distribution shows large difference between geometries. Larger and higher granularity geometry apparently gives better results in π^0 reconstruction.

Table 3 shows a result of selection efficiency and purity for each detector geometry. For $\tau^+ \rightarrow \rho^+ \nu_\tau$ mode, both results of selection without π^0 invariant mass cut and selection with

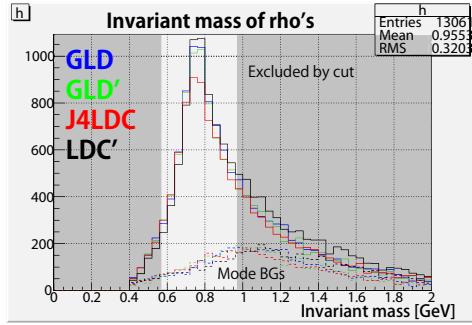


Figure 2: Invariant mass distribution of ρ with four geometries.

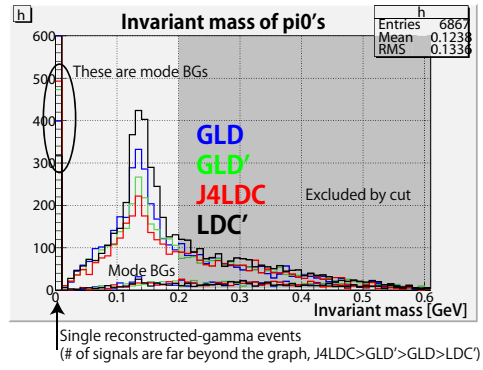


Figure 3: Invariant mass distribution of π^0 with four geometries.

Geometry	gldapr08_14m	gldprim_v04	j4ldc_v04	LDCPrime_02Sc
π mode efficiency	21.3%	21.4%	21.4%	21.2%
π mode purity	85.7%	83.6%	80.8%	88.5%
ρ mode eff. wo/ π^0 cut	12.7%	12.1%	11.3%	12.8%
ρ mode pur. wo/ π^0 cut	83.4%	81.8%	81.4%	85.7%
ρ mode eff. w/ π^0 cut	5.31%	4.32%	3.72%	6.38%
ρ mode pur. w/ π^0 cut	92.3%	90.3%	90.5%	93.9%

Table 3: Selection efficiency and purity for polarization analysis.

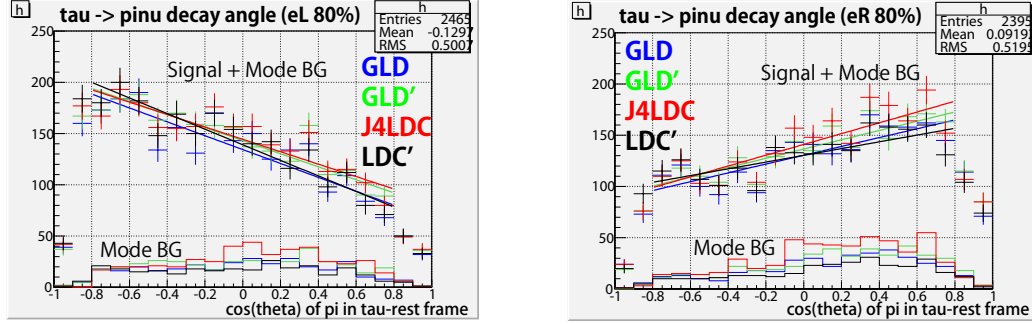


Figure 4: Angular distribution of charged pion in tau-momentum frame, left: $e_L^- e_R^+$ polarization, right: $e_R^- e_L^+$ polarization.

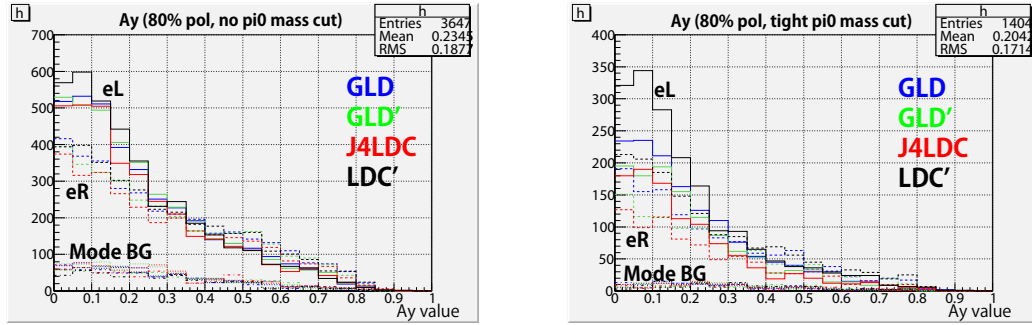


Figure 5: Distribution of parameter y . See text for details of y . left: mode selection without π^0 invariant mass cut, right: selection with π^0 mass cut.

π^0 invariant mass cut are shown in parallel. π^0 mass cut gives higher purity in event selection but efficiency becomes much less, thus the cut seems not practical for analysis in current geometries. For all selection LDCPrime.02Sc gives the best result, and gldapr08.14m follows the next.

5.2 Polarization measurement

To obtain polarization of $\tau^+ \rightarrow \pi^+ \nu_\tau$ events, $\cos\theta$ distribution of pion momentum direction with respect to tau momentum direction should be observed.

Figure 4 shows the $\cos\theta$ distribution. For the $e_L^- e_R^+$, number of events is larger in $\cos\theta < 0$ area, and for the $e_R^- e_L^+$, number of events is larger in $\cos\theta > 0$ area. Polarization of tau leptons can be determined by the ratio of number of events between left and right half of the graph, or by linear fit of the histograms. Analysis shows the polarization can be determined by 1.2-1.3% statistical error, but the amount of remaining background varies by geometries as a result of difference in selection purity (for detailed numbers, see the slide[1]).

For analysis of $\tau^+ \rightarrow \rho^+ \nu_\tau$ polarization, analysis is more complicated. To obtain polarization of tau leptons, we can use ρ polarization, indicated by angular distribution of $\rho^+ \leftarrow \pi^+ \pi^0$ decay, in addition to ρ angular distribution with respect to τ frame. To com-

bine those indicator, we use y parameter, defined in [3] as

$$y = \frac{E_{\pi^0} - E_{\pi^+}}{E_\tau}. \quad (3)$$

According to [3], polarization of tau leptons can be determined by

$$0.85P_\tau = \frac{N(y > y_c)}{N(y > y_c; P_\tau = 0)} - \frac{N(y < y_c)}{N(y < y_c; P_\tau = 0)}, y_c = 0.316. \quad (4)$$

Figure 5 shows the y distribution. From the distribution, P_τ can be determined by 1.1-1.2% statistical error if we do not apply π^0 mass cut, and 1.7-2.3% with π^0 mass cut (again, detailed number can be seen in the slide[1]). Difference can be observed between geometries, due to selection efficiency, but with no π^0 mass cut the difference is not so large.

6 Summary

Tau-pair process has been analyzed in the ILD detector models. It is found that tau-pair forward-backward asymmetry observation of better than 1% resolution can be achieved in the current ILD detector models and no large difference between detector models are found. For the polarization analysis, clear dependence is seen in π_0 reconstruction. LDCPrime_02Sc gives the best result and gldapr08_14m follows. With the result we can estimate that larger and more granular detector models give better results.

References

- [1] Presentation:
<http://ilcagenda.linearcollider.org/contributionDisplay.py?contribId=167&sessionId=17&confId=2628>
- [2] The WWOC Software panel: T. Behnke, N. Graf and A. Miyamoto, ILC-MEMO-2008-001
- [3] K. Hagiwara, A.D. Martin and D. Zeppenfeld, Phys. Lett. B. **235** 198 (1990).